Research Developments in Wood Engineering and Technology

Alfredo Aguilera
Universidad Austral de Chile, Chile

J. Paulo Davim
University of Aveiro, Portugal

ENGINEERING SCIENCE REFERENCE
An Imprint of IGI Global

Managing Director: Lindsay Johnston
Production Manager: Jennifer Yoder
Publishing Systems Analyst: Adrienne Freeland
Development Editor: Allyson Gard
Acquisitions Editor: Kayla Wolfe
Typesetter: John Crodian
Cover Design: Jason Mull

Published in the United States of America by
Engineering Science Reference (an imprint of IGI Global)
701 E. Chocolate Avenue
Hershey PA 17033
Tel: 717-533-8845
Fax: 717-533-8661
E-mail: cust@igi-global.com
Web site: http://www.igi-global.com

Library of Congress Cataloging-in-Publication Data

Research developments in wood engineering and technology / Alfredo Aguilera and J. Paulo Davim, editors.
pages cm
Includes bibliographical references and index.
Summary: “This book examines the latest research advances and technological developments for wood material as an engineering product and the innovation it provides for environmental friendly materials”-- Provided by publisher.
ISBN 978-1-4666-4554-7 (hardcover) -- ISBN 978-1-4666-4555-4 (ebook) -- ISBN 978-1-4666-4556-1 (print & perpetual access) 1. Wood. 2. Wood--Testing. I. Aguilera, Alfredo, 1964-, editor of compilation. II. Davim, J. Paulo., editor of compilation.
TA419.R37 2014
620.1’2--dc23
2013020528

British Cataloguing in Publication Data
A Cataloguing in Publication record for this book is available from the British Library.

Chapter 7
3D Non-Destructive Evaluation Techniques for Wood Analysis

M. Paulina Fernández
Pontificia Universidad Católica de Chile, Chile

Iván Lillo
Pontificia Universidad Católica de Chile, Chile

Cristian Tejos
Pontificia Universidad Católica de Chile, Chile

Andrés Guesalaga
Pontificia Universidad Católica de Chile, Chile

Gerson Rojas
Universidad del Bío-Bío, Chile

Pablo Irarrázaval
Pontificia Universidad Católica de Chile, Chile

ABSTRACT

Non-destructive testing techniques allow the analysis of wood characteristics without altering its end-use capabilities. Wood morphology, wood density, moisture content, and wood decay are some of the features detectable by means of different non-destructive methods. Among them, Computed Tomography (CT) and Magnetic Resonance Imaging (MRI) stand out because of their ability to measure information in a three-dimensional fashion. This enables one to scan volumetrically an entire tree log, giving measurements of each location of the analyzed volume. The output data can provide information about internal structures or physiological features, which can then be used for optimizing industrial processing or for research purposes. In this chapter, the authors describe CT and MRI in terms of their operational principles, sampling conditions, data outputs, and advantages and disadvantages.

DOI: 10.4018/978-1-4666-4554-7.ch007

INTRODUCTION

Wood is a matter of biological origin whose appearance and properties commonly deviate from what is considered desirable. The presence of pith, knots, fiber misalignment, resin pockets, cracks and wood alterations such as rot, color and other abnormalities generated during growth, determine the quality of the lumber and consequently its final value. Generally, the commercial value of the lumber is inversely related to the amount and size of those defects (Sarigul et al., 2003). Due to the increasing demand for higher quality lumber coming from logs felling, forest companies are devoting a significant effort to optimize log breakdown, sawing and peeling. Optimizing those processes can improve productivity, decrease production costs and improve recovery value. Productivity in sawmills mainly depends on the features of the raw material, the final product valuation, the type of technology employed, the maintenance of cutting devices and tools, operators training level, among other factors. Considering that raw material cost can account for more than 75% of the total production cost (Steele et al., 1992), an optimal log recovery is crucial for the profitability of the wood industry.

Currently, sawmills employ computing software to optimize cutting patterns, based on input information related to main external features of the log such as diameter, length, taper, curvature, etc. These features can be measured before starting the sawing process using commercially available technology such as 3D shape scanners. Additionally, if internal defects were known, the process could be optimized in relation to log location just when the log is going to be cut (Harless et al., 1991). Certainly, knowledge of internal defects before sawing procedure would improve lumber quality and would increase its value. According to Steele et al. (1994), lumber value could increase in 10% depending on internal defects identification and optimal log location with respect to cutting patterns. Even though there are a few technologies that could reveal internal features and defects of the logs, the wood industry has not introduced those technologies as a common tool for cutting optimization. There are however some relevant prototypes (Microtec CT and 2DX Ray scanner (Microtec Tomolog)) which have been developed for this particular purpose and they are being assessed at laboratory and industrial levels in Europe.

The need to detect and characterize internal features and defects has motivated several research efforts focused in the development and evaluation of non-invasive testing techniques of log and lumber pieces.

According to the working party 5.02.01 – Non-destructive evaluation on wood and wood-based materials – of the International Union of Forest Research Organization (IUFRO) – a non-destructive evaluation (NDE) is the science of identifying the physical and mechanical properties of a material without altering its end-use capabilities and then using this information to make decisions regarding appropri-

ate applications. Such evaluations rely upon nondestructive testing technologies to provide accurate information pertaining to the properties, performance, or condition of the material in question (IUFRO Division 5 – Forest Products, 2012).

Non-destructive testing of wood has been recognized as an important field in wood technologies oriented to support research on wood properties and particularly to support evaluation tools during the breakdown of the log and the subsequent wood processing. These techniques aim at maximizing the yield of the raw material, together with a classification for the best end-use, and improving and controlling the quality of these final products. In the last 30 years an increasing amount of research and new technologies have been developed. Many of the measurement principles and technologies are inherited or adapted from medical applications for non-invasive diagnosis.

Some of the wood properties that can be evaluated by existing non-destructive testing technology are: density; elasticity; moisture content; fiber direction; presence of relevant features (knots, resin pockets, cracks, wood decay, rings, reaction wood, etc.); microfibrilar angle; heartwood and sapwood distinction; prediction of pulp yield, and chemical compounds (Bucur, 2003; Beall, 2007).

Non-destructive evaluation techniques can be classified according to: 1) the wood properties being evaluated (Beall, 2007); 2) the physical principles of the technique; 3) according to the scale of the wood component that can be analyzed (Bucur, 2003); or 4) according to the kind of output information.

Following the fourth criterion, non-destructive testing techniques can be classified as those that give information of some overall wood property (without spatial discrimination); those that give information for every location on a two-dimensional slice of the analyzed log; and those that give information for every location of an entire volume, i.e. a three-dimensional (3D) map that can show the measured variable of a volume, but discriminating on each spatial location of the analyzed log or lumber piece.

Some of the main techniques for industrial use or for research in solid wood are ultrasound (Bucur, 2003; Bucur, 2006; Ross et al., 1998; Leininger et al., 2001); acousto-sound (Bucur, 2006; Grabianowski et al., 2006; Raczkowski et al., 1999; Wang et al., 2009; Mahon et al., 2009; Li et al., 2012); microwave (Bucur, 2003; James et al., 1985; Johansson et al., 2003; Schajer & Orhan, 2005;); gamma rays, (Bucur, 2003; Tiita et al., 1996; Gierlik & Muchorowska, 2000; Karsulovic et al., 2005); X-ray Computed Tomography (CT) (Baumgartnert et al., 2010; Brüchert et al., 2008; Longuetaud et al., 2012); and Magnetic Resonance Imaging (MRI) (Wang & Chang, 1986; Araujo et al., 1992; MacMillan et al., 2001).

From all the existing non-destructive techniques, only two of them correspond to 3D imaging techniques: CT and MRI. Both techniques come from the medical area. They have different levels of development but they both show great potential,

as they allow three dimensional visualization and measurements of solid wood. Therefore, they are considered as promising techniques for industrial processes like sawmill, plywood and veneer mills.

In the following, we will present both techniques in term of their principles, applications in wood, 3D reconstruction of information, and we will discuss their potential for future industrial use.

CT SCANNER

X-Ray Principles

Discovered by William Röntgen in 1895, X-ray images have been commonly used in medical applications for more than a century. Basically, X-rays are electromagnetic waves (or "invisible light") at high frequency, capable of cross some materials and be attenuated by others. The image is created in a film, or by semiconductor devices to form a digital image (Novelline & Squire, 2004). Its physical principles are beyond this chapter, so they will be briefly summarized.

On the electromagnetic spectrum, X-rays are located between UV rays and gamma rays, with frequencies between $3x10^{16}$ and $3x10^{19}$ Hz. Commonly, two types can be distinguished: "soft" and "hard" X-rays. They differ in their ability to penetrate matter, and the physical conditions that produce them. The "hard" X-rays have a wavelength between 0.1 nm and 0.01 nm (greater than 10 keV energy), which is in the order of an atomic radius. Only "hard" X-rays have the ability to penetrate matter, so are used to generate X-ray images.

When X-rays pass through an object, ray intensity or flow decreases depending on the characteristics of the material. Typically, denser materials provide greater attenuation of the rays. In a human radiography image we can distinguish between bone and soft tissue, although what we see in the picture is the 2D projection of the attenuation of a 3D body part in the direction of the X-rays.

Under ideal conditions, attenuation in a homogeneous material under a constant source of parallel X-rays is expressed by the Beer-Lambert law (Prince & Links, 2006):

$$I = I_0 \exp(-\mu x) \tag{1}$$

Where I_0 is the incident intensity, μ the linear attenuation coefficient, x the material thickness and I the final intensity after crossing the homogenous body. The linear attenuation coefficient is related to the material composition and density, so

that in heterogeneous materials it is a function of the position and no longer a constant. The total attenuation measured at the receiver depends on the number of X-rays crossing the object, and characteristics of the object itself, like density and composition. Besides, other effects such as distortion of rays and the sensitivity of the receiver must be considered. The general form of Equation (1) summarizes all those effects. The image obtained by attenuation of X-rays is thus a weighted sum of the local attenuation, integrated across the entire object the rays pass through.

$$I_d(x,y) = \int_0^{\varepsilon_{\max}} \eta(\varepsilon) I_0(\varepsilon) \exp(-\int \mu(x,y,z,\varepsilon) dz) d\varepsilon \tag{2}$$

Where $\eta(\varepsilon)$ is the receptor efficiency at energy level ε. Since μ is not constant, the sum of local attenuation coefficients appears. The importance of the Equation (2) is the dependence of the image in terms of the receptor, the source, $(I_0(\varepsilon))$ and local attenuation characteristics of the 3D object in the direction of the X-rays. X-rays sources generally emit photons in wide spectra, thus emitted photons do not have the same energy. In this sense, X-ray sources are called polychromatic or polyenergetic.

Another consideration is noise in the images, due to quantum effects in the whole process. X-rays are highly energetic, so the number of photons leaving the emitter is very low compared to a visible light source with similar energy. Additionally, X-rays flux leaving the emitter is not uniform. As with visible light, photons generation can be modeled as a Poisson process. Other stochastic processes, modeled as binomial processes, are added when rays cross the object and hit the receiver. In general, if an object has low attenuation, the signal to noise ratio may be low, requiring a greater exposure to the rays to obtain a high quality image.

Under certain conditions, a linear relationship between the attenuation and the density of the material can be established, when the source is far from the object and receiver, and the density of the object does not vary in the direction of the rays, for example using a thin object. In wood, a high linear correlation between density and attenuation has been shown. In a well designed setup, X-ray densitometry could be computed from calibrated images (Cown & Clement, 1983).

Computed Tomography (CT)

Projection X-rays produce a 2D image from a 3D object. It is desirable to obtain an internal image of an object without destroying it. This is possible by means of computed tomography (CT), which is one of the fastest growing non-destructive techniques for the analysis of wood.

In CT, 1D projections are obtained from a small portion (slice) of the object, using collimators to direct rays through the slice. Digital receivers are located on the opposite side of the object. Each projection is the sum of the attenuation of the slice in the direction of the rays. In this way, is the same process of projection X-rays viewed as an image from the top of the slice: the resultant image will be a line in 2D, or the 1D projection of the slice. The system is rotated to get projections for multiple angles, finally obtaining a set of projections, typically hundreds, in a set of directions to complete a regular sequence. The image in CT is not gotten directly, but must be reconstructed using a mathematical algorithm (so called "computed"). CT images correspond to attenuation images as projection X-ray from 3D to 2D, but in a slice of object instead of the whole object. Figure 1a shows the generation of one 1D projection.

Figure 1. (a) 1-D projection from thin slice of 3-D object; (b) Philips CT-scanner, multi-slice processing a log at the image laboratory, Hospital del Trabajador, Concepción, Chile; (c) A Pinus radiata log digital image showing the presence of knots, heartwood, clear wood, and growth rings; (d) Pinus radiata log CT image (Rojas & Ortiz, 2012, with permission); (e) Eucalyptus nitens log digital image showing the presence of knots, bark, and grown ring; (f) Eucalyptus nitens log CT image.

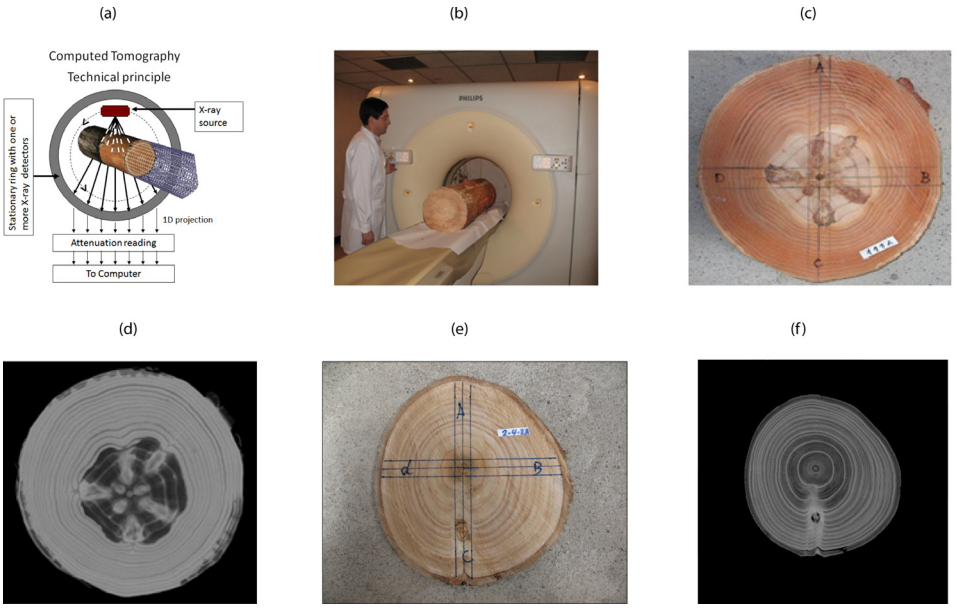

Image CT

Most common CT machines currently use several emitters (X-ray fan beam) and multiple detectors, to speed up the acquisition. As the detectors are digital, data is reconstructed on the fly. The final image depends on the number of 1D projections, the greater the number, the better image quality. It is also possible to use array detectors rather than linear, taking more than one slice at a time. CT remains the attenuation properties of the X-ray projection, and the remarkable ability of acquire an inner image of an object without destroying it; in a reasonable time and cost. This makes CT one of the preferred non-destructive inspection tools.

In the ideal scenario, where x-rays are unidirectional and the detector is straight, Radon transform can be used to obtain an accurate description of the 1D projection of the object slice (Kak & Slaney, 1988). For a particular angle, φ the projection is given by:

$$p_{\varphi}(r) = \int_{-\infty}^{\infty}\int_{-\infty}^{\infty} f(x,y)\delta(x\cos\varphi + y\sin\varphi - r)dxdy \tag{3}$$

Where $f(x,y)$ represents the 2D object slice attenuation represented in the image. In this ideal case, what is obtained with CT is the Radon transform for continuous values of φ among $\left[0,\pi\right]$ and r between $(-\infty,\infty)$. From the projections, $f(x,y)$ could be estimated (or reconstructed) by inverting the Radon transform. The reconstruction is not trivial; so many algorithms have been developed (and still developing). For direct reconstruction, the better is filtered back projection, using the central section theorem, which uses Fourier transform.

In practice, direct reconstruction methods are used to obtain a first approximation of the reconstruction, where a more sophisticated reconstruction algorithm performs back end. The issues for direct reconstruction are related to the use of non-parallel rays, the geometrical arrangement of the detectors, the finite number of projections, the sampled nature of digital 1D projections, among others.

Modern CT scanners provide a high quality/resolution image of slices of objects. 3D images are obtained by stacking 2D images, and with new emitter/detector arrays. In general, getting an image in a CT scanner is fast compared to other techniques as MRI, with typical acquisition time in order of seconds.

Computed Tomography (CT), which was developed to be used in medical science, is the most popular non-destructive method that has been employed for wood analysis. In this sense one of the main applications of X-ray CT has been particularly associated with the internal assessment of logs and identification of characteristic features.

For example Figures 1c and 1d present a radiata pine log digital photo and the original CT image, respectively. Visual examination of Figure 1d shows clearly the internal characteristics such as knot, heartwood, clear wood, and growth rings. These characteristics appear as light or dark zones (respectively of high or low density) or as discontinuities in the normal growth ring patterns of the log. Knots can be easily identified by their whiteness (due to denser wood), by their elliptical form and by the change in wood grain occurring in the vicinity of the knot. Heartwood generally shows a circular shape and dark color, mainly due to lower MC and concentrations of inorganic and extractive substances. Nonetheless, a variation in grey level across growth rings can be observed inside the clear wood area. This is basically related to the density difference existing between early wood and late wood which is part of the tree growth rings. Besides, there is a certain level of noise in the log peripheral area which is mainly due to the decrease of the moisture content because of lack of bark. This condition can be explained because of the CT scanner physical principle: the information obtained from a CT image is related to log green density which is sensitive to moisture content variation.

Applications of CT-Scanner on Wood

At the beginning the goal of studies using Computed Tomography was to check the ability to identify in obtained CT images main log internal defects. An automatic system for CT image segmentation with the purpose of identifying knots and be able to measure perimeters in *Pinus ponderosa* logs and *Quercus rubra* logs was developed by Taylor et al. (1984). This method, based on the analysis of grey levels of CT images obtained from histograms of intensity and frequency made possible the identification of knots and the external shape of logs. However, according to researchers reports due to log moisture content and scarce density variation in the area where the knot was located and the area around the knot it was very difficult to identify and locate such targets with more accuracy. Funt and Bryant (1987) developed a software to identify internal defects such as knots, rot and cracks in logs of hemlock, Cedar and Douglas-fir with the use of CT images. The computer program uses the high density and elliptical shape of knots to distinguish them from clear wood, and the low density and rouge texture of rotten areas to separate rotten wood from sound wood. Results showed that CT images can be translated by the software and that internal defects can be accurately identified. Wagner et al. (1989) reported that internal defects in Oak logs could be identified from images obtained from computed tomography. More recently, Rojas et al. (2005) reported it is possible to identify internal defects in CT images of green Sugar maple (*Acer saccharum*) logs but identification gets complicated when there is a large variation

in moisture content inside logs. In general most of these methods present only a qualitative evaluation of their detection procedures performance.

In addition, prediction of knot internal parameters has been determined by X rays computed tomography. For example, Björklund (1997), Björklund and Petersson (1999), Moberg (2000), and Oja (2000) are some of the researchers which have done work on this subject. Oja & Temnerud (1999) reported about a study carried out to identify resin pockets in CT images coming from *Picea abies* green logs. Results showed that it is possible to identify resin pockets with this particular method. However, according to these researchers there is a large difference in grey levels when sapwood is compared to heartwood mainly because of the difference in moisture content.

In this direction, Figure 2 shows a series of CT images obtained for the cross-section of Sugar maple logs (*Acer saccharum*) after 0, 2, 6, 10 and 14 weeks of felling. Figure 2a shows the presence of knots, colored heartwood, sapwood and bark. Figures 2b, c, d, e show variations in the gray level while log drying is taking place. When figures 2a and 2e are compared visually, it can be observed that the sapwood zone presents more variation in the gray level than the colored heartwood zone, knots and bark.

3D Reconstruction of Wood

In another sense, 3D reconstruction of logs internal features from CT images (2D) has also been explored. A prototype vision system for analyzing and imaging of hardwood was developed by Zhu et al. (1996). This vision system locates and automatically identifies internal defects in hardwood logs. First, this system filters CT images (2D format) to remove useless details, then it makes segments from CT images with the purpose of separating possible wood defective areas from non-defective wood and finally, with CT images (2D) already segmented it rebuilds a three-dimension image (3D). Preliminary tests performed on Southern red oak logs and Yellow poplar logs showed that internal defects identification is possible using the vision system based on CT images. Nevertheless, main system limitations are related to moisture content variation of logs and to system operation speed.

Besides, Bhandarkart et al. (1999) developed a vision system (CATALOG) which detects and builds 3D images of most relevant internal defects such knots, cracks and resin pockets. This particular system divides CT images in segments (2D format) to separate wood defective areas from sound wood and then it rebuilds a 3D image of the log where internal defects can be observed. According to the former researchers CATALOG, does not get good results with CT images which contain defects or irregular or too dense growth rings, or where rings width is less than scanner space resolution. Besides, CT images showed a low level of density variation when

Figure 2. Typical CT images of one cross-section of sugar maple log (Acer saccharum) showing the presence of knots, colored heartwood, central split, bark, and sapwood. The sequence shows the effect of desiccation on image signal, after felling and then after different clatter on. This CT image was obtained from a Siemens Somatom X-ray CT scanner at the Natural Resource Scanography Laboratory owned and operated jointly by the Institut National de la Recherche Scientifique, Forintek Canada Corp., and Université Laval in Quebec City, Canada.

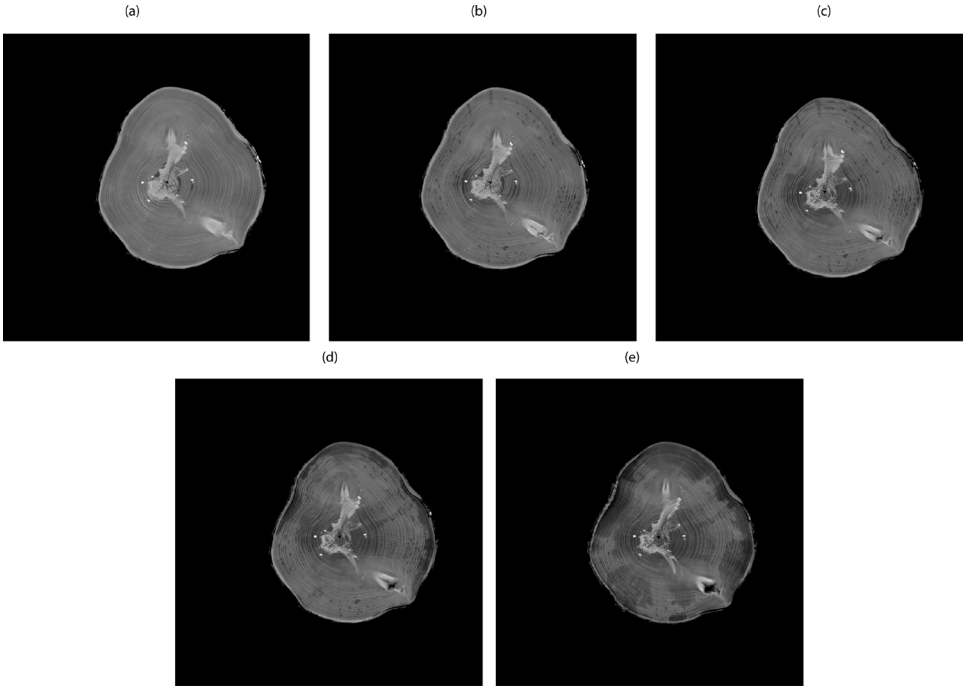

normal wood and defective wood were compared. In this direction, Bhandarkart et al. (2006) they described the design and implementation of a computer vision system for the detection, localization, and 3D reconstruction of internal defects in hardwood logs from cross-sectional CT images. This approach proposed integrated defect detection, defect localization, and 3D defect reconstruction by incorporating a Kalman filter-based feature tracking scheme. The detection rate for all the tested species was of a 100%. For cracks and holes, the values varies between 95 and 100%.

Brüchert et al. (2008) scanned *Picea abies* logs with a discrete two level X-ray scanner and after re-scanner with a CT scanner. From obtained CT images 3D model taken from logs were rebuilt with the purpose of measuring growth rings width. Results were compared with obtained measurements from a two level X-ray scanner. In general, wood features can be detected and measured with a high level of

accuracy. Nevertheless, there were a large number of local missing values along the length of a log due to wood heterogeneity. Wei et al. (2009) employed the method based on the marching cubes algorithm to generate a 3D reconstruction of internal features (heartwood, sapwood, bark, and knots) of *Acer saccharum* pieces and *Picea mariana* pieces from CT (2D) images. According to these authors the suggested method generates very clear 3D images of each internal feature, except for the knots, which have a roughness level. This last may be caused by the high thickness of slice (10 mm). Baumgartner et al. (2010) scanned *Pinus sylvestris* logs in a CT scanner (Microtec CT Log). Obtained images were used to get three-dimensional shapes of knots (3D) with the purpose of identifying knots present in the heartwood. Obtained results showed that knot direction and size can be identified with a high degree of accuracy using 3D shapes obtained from CT images. However, these authors stated that the shape of the knot which is present in the sapwood is difficult to separate due to the small difference between knots grey level and sapwood. Recently, Longuetaud et al. (2012) developed an algorithm to automatically detect and measure knots in CT images of *Picea abies* and *Abies alba*. This algorithm is based on the use of 3D connex components and a 3D distance transform. The main results obtained showed detection levels between 71% and 100%.

In general, according to reviewed literature, it is clear that Computed Tomography is a non-destructive method which permits the identification of defects and internal features of logs. Quantitative analysis concerning detection accuracy of different classification methods or CT images segmentation presented for different types of wood let us view the large potential of this non-destructive technique for sawmill industry. To previously know the location, number and type of internal defects before starting the sawing process would assist in software optimization or cutting patterns improvement in sawmills and it would consequently increase volumetric utilization of transformation process. However, the problem is not completely solved. Wood complex structure and its inherent variability, density and moisture content variations limit in some cases accuracy in internal defects identification. Likewise, and according to some researchers, reconstruction of 3D images from CT images obtained from computerized tomography would permit the collection of more information with respect to log internal features. This situation encourage researchers to go on working and assessing different image processing methods and 3D modeling, which will provide more accuracy in internal defects identification.

MAGNETIC RESONANCE IMAGING (MRI)

MRI Principles

An MRI scanner consists of a strong homogeneous magnetic field (B_0); a set of gradient coils and Radio-Frequency (RF) coils (Figure 3a). The most common element detected by MRI scanners is the single proton Hydrogen (^1H) that acts as a small magnet dipole, referred as spin. Without an external magnetic field, nuclear spins are oriented in random directions. The acquisition of an MR image requires four steps: polarization, excitation, readout and reconstruction (Figure 3a). The object is polarized introducing it into the bore of a superconducting magnet (Figure 3b), which produce a strong homogeneous magnetic field. The spins precess about the direction of the main magnetic field B_0, at a specific frequency (Larmor frequency). The individual contribution of each spin produces an overall magnetization in the direction of B_0 (longitudinal direction). During the excitation, an RF coil is switched on producing a rotating magnetic field B_1, in the direction transverse to B_0. This rotating field tips the magnetization out of the longitudinal direction, as spins tend to follow B_1. A 90º excitation RF pulse makes the spins to precess in the transverse plane (Figure 3a).

Subsequently, the RF coil is switched off and the spins smoothly align themselves back to their equilibrium orientation, the longitudinal direction. This relaxation process can be analyzed with two components: the decay of the transverse component and the recovery of the longitudinal component of the magnetization. The speeds in those transverse and longitudinal components are determined by the time constants T_1 and T_2, respectively. The magnitude of T_1 and T_2 are inherent physical properties of each material. The variations of the transverse and longitudinal components of the magnetization are described by the equations:

$$M_{xy}(t) = M_0 e^{-t/T_2} \tag{4}$$

$$M_z(t) = M_0(1 - e^{-t/T_1}) \tag{5}$$

Where t is time, M_{xy} is the magnitude of the transverse magnetization, M_0 is the initial longitudinal magnetization and M_z is the magnitude of the longitudinal magnetization.

During the readout stage, the transverse component of the magnetization induces a voltage on an RF receiver coil, which is digitally recorded. The excitation and readout processes must be repeated several times in order to create a single image. Once all voltage signals are recorded, a standard reconstruction consists of apply-

Figure 3. (a) Schematic image of the MRI functional steps (see text for explanation); (b) magnetic resonance scanner at the Biomedical Imaging Center, Pontificia Universidad Católica de Chile; (c) 3D schema of a wood volume showing wood cells lumens differences of early and latewood and the effect on water holding capacity; (d) MRI cross section of a Pinus radiata sample (softwood or conifer species) showing earlywood (high signal, white and light gray tones) and latewood (low signal, dark to black tones). The darker lines permit to identify the limits between a wood ring and the following one. (e) MRI cross section image of Eucalyptus globulus sample (hardwood – broadleaf species) showing a more diffuse ring structure given their capacity to growth all around the year. The dark spot at left of the center corresponds to a branch. In both samples, the bright signal (white color) in the peripheral sector corresponds to very active cambial tissue and enlarging wood cells area.

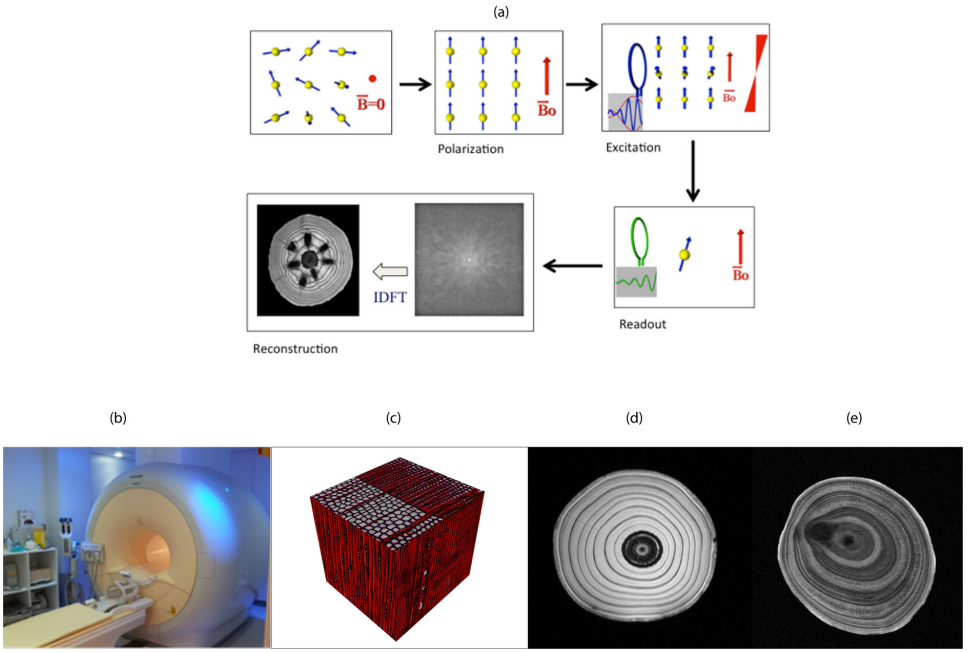

ing an Inverse Discrete Fourier Transform (IDFT) to the signals and the image is ready to be displayed. Data can be acquired in a three-dimensional fashion; therefore entire volumes can be analyzed.

MRI allows the generation of image contrast as a function of several properties present in the scanned object such as ^{1}H proton density (ρ), longitudinal relaxation time constant (T_1) and transverse relaxation time constant (T_2), among others. Different acquisition strategies and parameters allow different element properties to

Table 1. T_1 weighted (T_1-w), T_2 weighted (T_2-w) and proton density repetition time T_R and the time of echo T_E in relative values

MR image	TR	TE
T1-w	Short	Short
T2-w	Long	Long
Proton density	Long	Short

be encoded by the image contrast. For standard MRI scans, the most important contrast-related acquisition parameters are: the repetition time T_R, which is the time interval between two consecutive excitation processes; and the time of echo T_E, which is the time between the excitation and readout (within the same T_R). Choosing relatively short T_R and T_E's will generate an image in which intensity differences of two pixels reflect differences in the T_1 values of the elements contained in each pixel. This is called a T_1-weighted (T_1-w) MR image. Equivalently, other combinations of T_R-T_E values generate proton density-weighted (PD or ρ) or T_2-weighted (T_2-w) MR images (Table 1).

Formally, the pixels' intensity (A_E) of a standard MR image can be modeled by the expression:

$$A_E = \rho(1 - e^{-T_R/T_1})e^{-T_E/-T_2} \tag{6}$$

From Equation 6, it is clear that it is not trivial to select optimum acquisition parameters, particularly for wood, because T_1 and T_2 are unknown a priori. It is therefore necessary to find those acquisition parameters heuristically.

Other physical or physiological phenomena can be also observed with MRI using slightly different acquisition strategies. This includes diffusion processes; magnetization transfer; resonance spectrum (spectroscopy); magnetic susceptibility, among others (Hashemi, 2004; de Graaf, 2007).

Other important imaging-related issues are Signal to Noise Ratio (SNR) and image resolution. Since most of the MR signal comes from water, the moisture content of the samples is critical; the higher the moisture content, the better the image will be. Therefore, time interval between harvest and imaging needs to be short, and samples needs to be protected from moisture loss (Nishimura, 1996).

MRI Applications in Wood

According to Eitelberger et al. (2011) water can be present in wood in three different phases: as bound water, which corresponds to water molecules located within

the cell walls; as free or "bulk" water, which corresponds to water molecules in the cell lumen; and as water vapor. Below the fiber saturation point only bound water and water vapor exist to a significant extent. Dvinskikh et al. (2011) indicate that molecules from bound water have lower activity, slower molecular dynamics, they form hydrogen bonding to macromolecules, and apparently, they lack the transition phase of freezing in comparison to free water. Thus, MRI parameters can be set to emphasize the hydrogen that is found in the free or "bulk" water, given their longer relaxation times as compared to hydrogen nuclei in woody fibers (Coates, 1998). Jones et al. (2012) report numerous studies of relaxation time distributions in wood revealing multi-modal patterns that represent water in different structural environments. The distribution includes slowly relaxing components (T_1 and T_2 around 100ms) and one or more fast relaxing components (T_1 and T_2 around 1-10 ms).

Wood cells are not homogeneous in size or in cell wall thickness. Growth rings are recognized due to the alternate bands of earlywood (developed during the first part of the growing season) and latewood (developed during the last part of the growing season) (Haygreen & Bowyer, 1996). Earlywood cells have a larger lumen and a thinner cell wall than those of the latewood cells. The water content variation in wood can be exploited to show MR images of these structures or of other relevant information. The presence of bulk water is common, for instance, in recently harvested logs. In this case, low density regions such as earlywood, with larger cells lumens and thinner walls, present higher water holding, higher water conduction capacity, and therefore higher signal when analyzed with MRI (Figure 3c). Similarly, wood of branches, with higher densities than the surrounding tissues, are shown with enough contrast so that to distinguish knots (Figure 4a,b,e,f). Low water content of resin pockets, or internal holes and cracks without tissue, can be easily recognized because of their almost lack of MR signal (Figure 4l,n,o). Heartwood can be recognized as a central core without signal, but in this case, the information of the inner rings gets lost.

The first MRI experiments on wood exploited differences in water content to study morphological characteristics of different species. Some of the most relevant research works with this focus are Hall et al. (1986) in *Populus tremuloides*; Wang and Chang (1986) in *Prunus serotina*; Chang et al. (1989) in *Quercus alba* and *Prunus serotina*; Flibotte et al. (1990) in *Thuja plicata*; Olson et al. (1990) in *Quercus alba*; Pearce et al. (1994) in *Acer pseudoplatanus*; Coates et al. (1998) in *Quercus velutina*; Merela et al. (2005) in *Fagus sylvatica*; Oven et al. (2011) in *Carpinus betulus*, *Fagus sylvatica*, *Picea abies* and *Quercus robur*; Contreras et al. (2002), Albornoz (2003); Morales et al. (2004) and Llanos et al. (2010) in *Pinus radiata* among others. The studies reported the observation of sapwood-heartwood, wood rings, earlywood-latewood inside of each ring, knots, wood rays, reaction wood,

Figure 4. Different images showing morphological structures of wood obtained mostly from proton density MR images. (a) Cross section of a cluster of 5 branches at different positions; (b) cross cut of a cluster of pruned branches; (c) cross cut of a young stem showing the needle traces as radial lines; (d) cross cut showing low signal in the center. The lack of water content permits to associate it with heartwood; (e) radial cut showing a branch profile; (f) radial cut of a pruned branch showing the recovery of wood after pruning, with a slight scar of occlusion; (g) radial cut showing the needles traces as short horizontal lines; (h) blue stain produced by fungal attack appears when wood lose water. In this image the lack of signal was absolutely coincident with the visual detection of blue stain in the sample; (i) tangential cut showing several knots; (j) tangential cut of a pruned branch showing the occlusion scar; (k) tangential cut showing also the needles traces as the typical freckles in wood; (l) cross section showing cracks as two linear zones lacking signal; (m) cross section of a cluster of cones just under formation; (n) cross section of a cluster of cones formed years ago, showing the empty holes produced by the expansion of the stem pushing the cones outside; (o) radial cut showing the same phenomena; at the right the border of the cone can be recognized by some brighter points in the dark surrounding of the stem. (All images correspond to Pinus radiata samples, taken at the Biomedical Imaging Center of the Pontificia Universidad Católica de Chile, with a 1.5 T MR scanner).

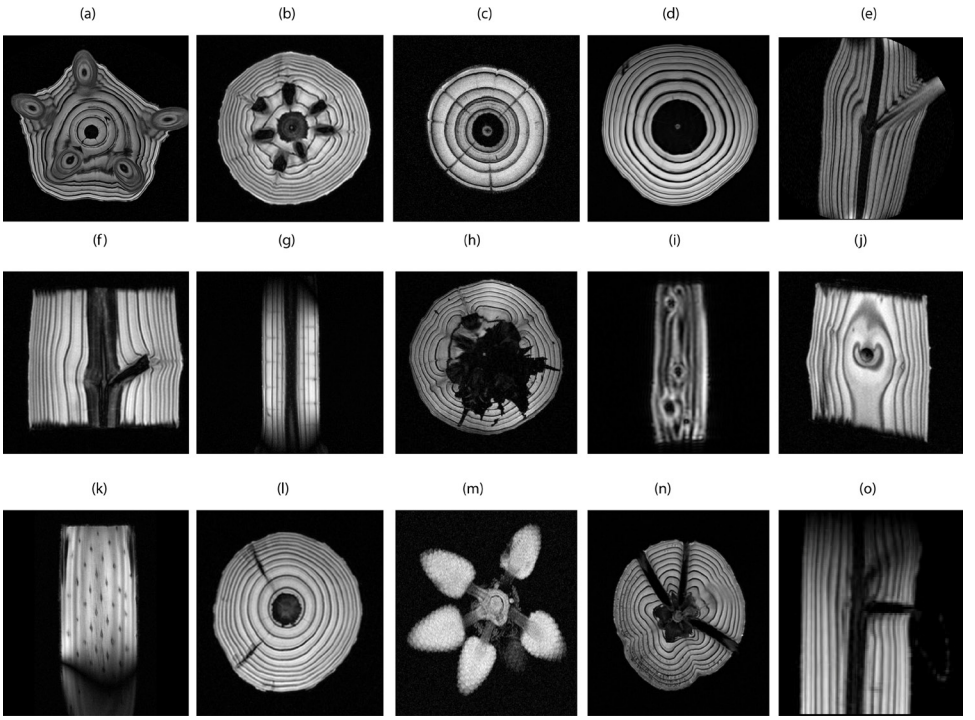

pith, needle traces, wet-wood, gum spots, wounds and cracks and wood decay identification, as can be seen in Figure 4 for *Pinus radiata*.

MRI technology has been also used to perform physiological studies in many species and tissues. Xylem and phloem flow in vivo, diurnal patterns of solute flow, embolism mechanism and repair, structure-function relationships among others, are part of the studies developed by mean of MRI (Borisjuk et al., 2012; Homan et al., 2007). Those studies include different species, for instance Veres et al. (1991) in *Blechnum unilaterale*; Araujo et al. (1992) in *Picea glauca*; Ilvonen et al. (2001) in *Pinus sylvestris*; Meder et al. (2003) in *Pinus radiata*; van Houts et al. (2004) in *Pinus taeda*; Terskikh et al. (2005) in *Pinus monticola*; Utsuzawa et al. (2005) in *Pinus thunbergii*; Kuroda et al. (2006) in *Pinus densiflora*, *Quercus serrata* and *Quercus crepuscula*, among others.

The ability of visualizing water dynamics in wood has also transformed MRI as a useful research tool for industrial applications. MRI has been recognized as the premier method for investigating water distribution in wood (Araujo et al., 1992; Bucur, 2003). It has been used for water motion analysis when drying or during water uptake of wood; to determine the different water phases in wood, water paths, embolism, among other applications.

Araujo et al. (1992) demonstrated that the spin-spin (T_2) relaxation behavior in wood is a continuous spectrum of relaxation times. The spectra of T_2 for *Picea glauca* show separate peaks corresponding to the different water environments. Bound water shows a peak with a T_2 of about 1 ms and lumen water shows a distribution of T_2 in the range of 10 to 100 ms. The T_2 of lumen water is a function of the wood cell radius. Consequently, different cell lumen radii distributions for sapwood, juvenile wood and compression wood can be readily distinguished. The T_2 behavior of lumen water in wood with moisture content over the fiber saturation point allows getting information about wood anatomy. As wood anatomy is related to wood density, with a proper analysis MRI could deliver information not only about water density but also about wood density. Complementary to that, the T_2 of bound water above saturation point scales as the solid wood density, because of homogeneous distribution of bound water inside of cell wall. Since bound water can be separated from free water, the behavior of water during wood drying can be followed in an MR image, giving an insight of the process. This could help in industrial kiln drying process monitoring and programming.

Ekstedt et al. (2007) used MRI to measure the uptake and loss of water from wood exposed to the environment, and also to test the relationship between coated wood and water exchange. At low moisture content conventional MRI cannot detect enough signals. Araujo et al. (1992) found that 17% was the lowest moisture content for a standard image acquisition. MacMillan et al. (2001) showed that woods with low moisture content could be visualized using more appropriate MRI sequences,

such as SPRITE (Single Point Ramped Imaging with T_1 Enhancement). Some examples showing MRI as a successful tool to study changes in water distribution during water uptake and drying are shown in Menon et al. (1989); Quick et al. (1990); Rosenkilde and Glover (2002); and Meder et al. (2003).

Dvinskikh et al. (2011) used samples that adsorbed heavy water (D_2O) to obtain spatial distributions of water content and the macromolecular wood tissue density. The experiments validated MRI as a tool for obtaining accurate and high-resolution measurements of moisture concentration gradients (and therefore diffusion mechanisms), and for observing the effects of chemical cell wall modification on moisture as well as details of molecular scale interaction between bound water and the polymers in the cell wall.

Another important industrial problem is wood decay in any of its developmental stages. Since pathogen presence increase when water content fall under the fiber saturation point, MRI can be used in the detection of pathogen damage (mainly due to fungi) by looking at the moisture content in wood. Pearce et al. (1994, 1997) analyzed pathogen damage in *Acer pseudoplatanus* and Müller et al. (2001) in *Fagus sylvatica*. We detected blue stain in *Pinus radiata* (unpublished data) in logs after a traditional sequence of harvesting, transporting and arrival to the mill (Figure 4h). On living trees, MRI has been used to understand how the tree reacts after being wounded (Pearce, 2000) and to detect the reaction zone because of its higher moisture content compare to healthy sapwood. Umebayashi et al. (2011) analyzed *Pinus thunberghii* wood embolism after inoculation with the wood nematode *Bursaphelenchus xylophilus*. The whole process of embolism and dysfunction of xylem is an important starting point to better understand the effect of wood wilt, silviculture management and posterior wood properties for the industrial drying or impregnation process.

3D Reconstruction

MRI is an intrinsic three-dimensional technique. Although one can choose to see a specific two-dimensional slice, data is normally acquired from an entire volume.

As in medical applications, the observation of a tree log needs to be done slice by slice, otherwise one would not be able to see all the internal structures of the tree. The advantage of having a 3D acquisition is that the orientation of the observed slices can be chosen a posteriori in any orthogonal or even oblique direction by means of a simple interpolation.

Some standard computer graphics algorithms could be applied to create a volumetric visual effect. Rendering or Maximum Intensity Projection (MIP) algorithms come already installed in the console of MRI scanners, and they can be used to look at structures as volumes, from different point of views. Importantly, creating a

volumetric visual effect always implies that one is choosing to observe a particular structure (e.g. the cortex, a particular ring, etc.) and discarding the rest.

A good example where rendering and MRI gives interesting results is in fiber tracking. MRI can be used to measure diffusion processes of fluids; this includes measuring Apparent Diffusion Coefficients (ADC) or even Diffusion Tensors (DT) on an entire volume. Looking at the preferable diffusion direction of an anisotropic diffusion process in each voxel of a DT image, one can define the path that follows the fibers of a tree log. We rendered those fibers to observe their shape and structure within the tree (Figure 5, unpublished work).

Key Problems to Solve

Although the great potential of MRI for research and industrial purposes, some practical problems still represent important limitations.

Wood loses water quite fast after tree felling or even in standing trees, as in heartwood formation (Figure 4d). Thus, the MRI signal dependence on water content becomes an important problem for industrial purposes. In an unpublished study we detected enough signals that allowed us to observe rings and other features with logs under 27% of water content, close to the 17% indicated by Araujo et al. (1992). We believe that there are still improvements that could be done in terms of sequence design using similar approaches as that used by MacMillan et al. (2001).

Figure 5. 3D fiber tracking in Pinus radiata

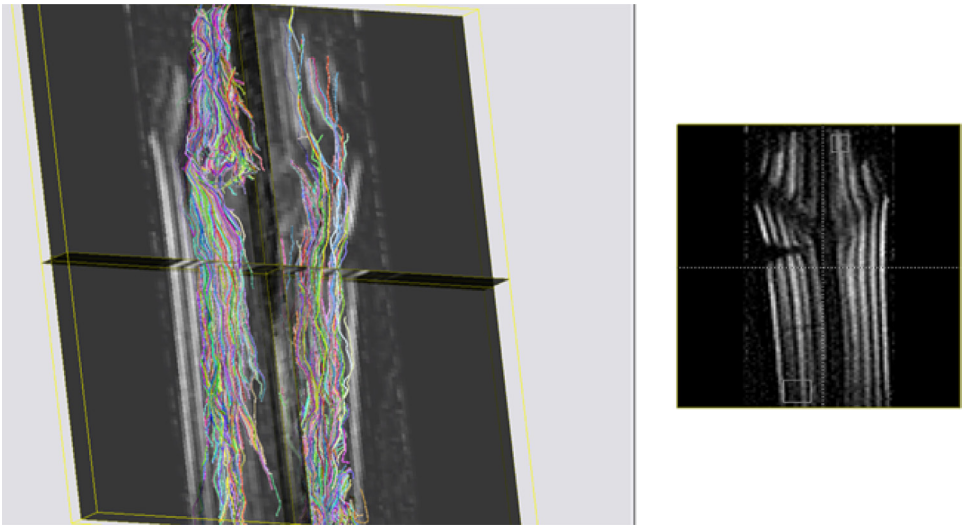

A second limitation is the relatively long scanning time needed in MRI. A standard 3D MRI scan of a large object could take several minutes. This is even more critical for low moisture content samples, since poor SNR forces to increase the total scanning time (by acquiring the same data set more than once and averaging together all the acquisitions) or to reduce the resolution of the image (therefore loosing image details) as seen in Figure 6. Some alternative approaches have been made in order to reduce the acquisition time without sacrificing image quality. Contreras et al. (2002) exploited the cylindrical symmetry of industrial logs by sampling them using transverse 1-D projections with an under-sampled helical pattern. The non-acquired data were estimated using linear interpolations and the imaging slices were reconstructed by filtered back projection. Computer simulations and experimental results showed that the method increased the scan speed by a factor of 6, while maintaining the ability to identify typical tree log characteristics.

Thinking in industrial applications, a third limitation arises in terms of the automation of the information extraction or processing from MR images. Coates et al. (1998) used region-growing methods on MR images of oak to segment defects from the surrounding normal wood and from growth rings. Although their interesting results, this technique—as they pointed out—shows some limitations since it requires the application of constant thresholds over images that sometimes do not have enough gray level variability. In those cases structures cannot be segmented properly. Morales et al. (2004) developed an algorithm for automatic recognition

Figure 6. Different time acquisition protocols and resolutions, showing the change on image quality

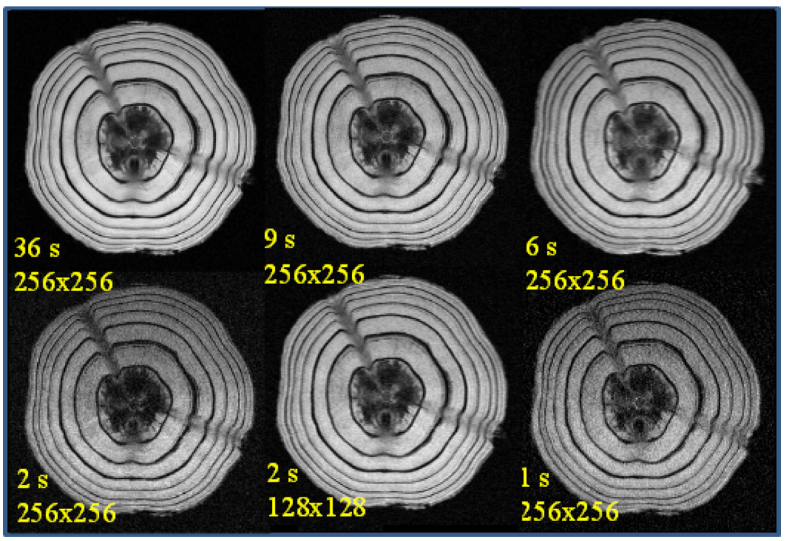

and reconstruction of rings. The algorithm analyzes a set of transversal MR images, detecting and reconstructing growth ring edges. By interpolation they obtained an accurate 3D reconstruction of the log and its fundamental constituents (individual rings, knots, defects, etc.), as seen in Figure 7. With such approach however, small structures could be lost as a result of the interpolation process. Although there are some successful examples (such as those previously mentioned), there are several image processing related problems that have not been solved yet for MRI. Most of the image-processing literature for wood reports algorithms for CT applications, which might not be easily translated into MRI applications.

Finally, size and portability are key issues yet to be solved in MRI. Image quality strongly depends on the strength of the main magnetic field. The technological solutions to produce strong and homogeneous magnetic fields have being oriented to the design of superconducting magnets. The resulting solutions imply having very large and heavy hardware that cannot easily transported, and therefore the current standard MRI technology cannot be used for outdoors or for portable applications.

Figure 7. (a) After log scanning, transversal information can be sampled and the profile of signal detected; by mean of a threshold the ring boundaries can be detected and the rings boundaries reconstructed. (b) 3D reconstruction of a log based on the automate rings detection algorithm developed by Morales et al. (2004).

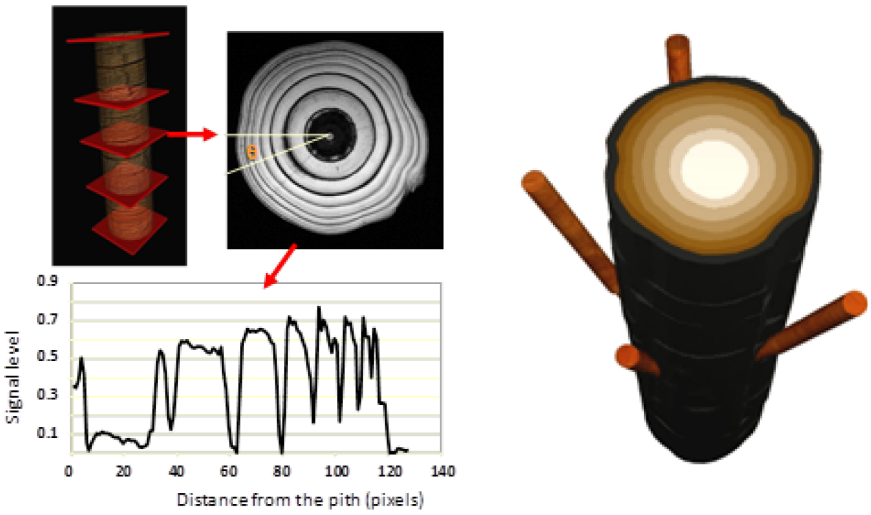

(a) (b)

New Developments

Different groups are working on portable MRI systems for outdoor plant studies. Okada et al. (2006) reported a portable 0.3 T scanner designed for outdoor measurements on maple trees. Kimura et al. (2011) continued the former equipment development, creating a flexible magnet-positioning system to measure healthy and diseased branches of Japanese pear tree in an orchard. Other authors have reported similar efforts for fruits measurements (Geya et al., 2013). Jones et al. (2012) presented the Tree-Hugger, a portable 1.1 MHz ^{1}H nuclear magnetic resonance imaging system with a 55 kg magnet of 0.026 T. They reported the measurement of a 90 mm diameter tree. Even though those kinds of solution represent major advances and useful tools for in-vivo pathological or physiological studies, the relatively low strength of their main magnetic fields inevitably produce important problems or limitations in terms of image resolution or SNR.

Outdoor-related problems (e.g. weather and temperature changes, dust, mud, etc.) are major restriction for the MRI hardware. Geya et al. (2013) and Van Has and van Duynhoven (2013) have shown some ongoing research and interesting results for fruits and other crops monitoring systems.

The health industry is the leading force behind MRI developments. In this sense, every year there are thousands of new developments in terms of hardware, sequence design and reconstruction that enable better quality or faster images, or the observations of different physical or physiological phenomena in the human body. Some of the recently developed advances enable to observe or measure diffusion processes, magnetic susceptibility, specific molecules, fiber tracks and other characteristics. Such developments have not been entirely translated into wood applications, and therefore, there is still a fertile ground for MRI research and development in wood.

DISCUSSION AND CONCLUSION

In general, X-ray Computed Tomography (CT) allows to identify and detect features and internal defects in wood such as growth rings, pith, sapwood, heartwood, knots, rot, cracks, and resin pockets, among others. It has been widely used for research purposes, but the precise identification and segmentation of features and defects can be affected by the variation of the moisture content of the pieces. Particularly, the sapwood's high water content absorbs radiation in a similar way as branch wood, decreasing image contrast and therefore ability of detecting knots in sapwood.

MRI appears as a versatile technique because of the broad kind of structural and physiological features that can be detected on wood. Morphological features, defects, water content, chemical compounds when applying spectroscopy, are the

most relevant variables. One of its major restrictions is the relatively high moisture content needed to obtain high quality images. Some advances have been done in order to get information at lower moisture content. Samples do not need a particular preparation, as far as water content is maintained preferably over the fiber saturation point. It means that logs coming directly from the forest or from the log yard could be processed, as also green sawn wood recently processed in the sawmill.

Both techniques are complementary in terms of the sample conditions needed for an appropriate data acquisition and the output information given by each one. The underlying physical principle in CT is the attenuation of X-ray photons, a phenomenon that strongly depends on the density (more precisely, the atomic mass) of the wood. Whereas for MRI, the ^{1}H-density, and therefore water content, is crucial for having enough signal on the images. If both techniques could be applied together in a log, they would give complementary information that could be integrated. This is a future line to explore.

Speed of MRI scans is slower than that of the main machine of a sawmill. This represents an important a limitation of the technique for its operative use in an industrial pipeline. A modern sawmill can process 70 to 120 longitudinal m of wood per minute, something that is far from what a standard high resolution MR image could take. There are some advances in reducing acquisition times using parallel acquisitions or using under-sampled reconstruction strategies, which could be evaluated.

Under a European Association of Research and Technology Organizations (EARTO) initiative (2012), the SP Technical Research Institute of Sweden in collaboration with Microtec, have developed a high resolution CT scanner for the forestry industry with fast data acquisition. The CT-Log (commercial name) was launched in September 2012. It is estimated that the system will significantly increase the profitability of the sawmill-to-final product chain by a 10%. The first scanners have been already used to find optimal cutting in a hardwood plant in the US, a veneer mill in Chile and a softwood sawmill in France. The producers expect that the time for a generalized adoption of the technology will be around 10 years.

CT and MRI are both expensive technologies. The profitability of these technologies for the forestry industry will depend on the level of recovery optimization that could be achieved when deciding the log breaking and processing utilizing information from the inside. Therefore this profitability also depends on the developments on optimization software for sawing processes.

As summarized in Table 2, both technologies are at different development levels, but both have a great potential for research and for the forestry industry. With the increasing interest in CT and MRI and the number of research initiatives that have recently started, we expect that this technology will be in the future a standard for the wood industry.

Table 2. Comparison between MRI and CT-scanner techniques considering their potential use in industrial process

	MRI	CT-scanner
Operative	No	Yes
Field work (in the forest)	Incipient work	No
Laboratory work	Yes	Yes
Time consumption	Large	Adequate for industrial purposes in new prototypes
Sample preparation	None	Dry
Costs	High	High

ACKNOWLEDGMENT

To FONDECYT (Fondo Nacional de Ciencia y Tecnología) of the Chilean Government, Projects N°11085008, N°1100864, N° 11060390 and Anillo ACT079

REFERENCES

Albornoz, J. L. (2003). *Magnetic resonance imaging of radiata pine logs*. (Thesis). Pontificia Universidad Católica de Chile, Santiago, Chile.

Araujo, C. D., MacKay, A. L., Hailey, J. R. T., Whittall, K. P., & Le, H. (1992). Proton magnetic resonance techniques for characterization of water in wood: Application to white spruce. *Wood Science and Technology*, *26*, 101–113. doi:10.1007/BF00194466.

Baumgartnert, R., Brüchert, F., & Sauter, U. H. (2010). *Knots in CT scans of scots pine logs: The future of quality control for wood & wood products*. Paper presented at the Final Conference of COST Action E53. Edinburgh, UK.

Beall, F. C. (2002). Overview of the use of ultrasonic technologies in research on wood properties. *Wood Science and Technology*, *36*, 197–212. doi:10.1007/s00226-002-0138-4.

Beall, F. C. (2007). Industrial applications and opportunities for nondestructive evaluation of structural wood members. *Maderas. Ciencia y Tecnología*, *9*(2), 127–134.

Bhandarkar, S. M., Faust, T. D., & Tang, M. (1999). CATALOG: A system for detection and rendering of internal log defects using computer tomography. *Machine Vision and Applications*, *11*, 171–190. doi:10.1007/s001380050100.

Bhandarkar, S. M., Luo, X., Daniels, R., & Tollner, E. W. (2006). A novel feature –based tracking approach to the detection, localization, and 3-D reconstruction of internal defects in hardwood logs using computer tomography. *Pattern Analysis & Applications*, *9*, 155–175. doi:10.1007/s10044-006-0035-9.

Björklund, L. (1997). The interior knot structure of pinus sylvestris stems. *Scandinavian Journal of Forest Research*, *12*, 403–412. doi:10.1080/02827589709355429.

Björklund, L., & Petersson, H. (1999). Predicting knot diameter of pinus sylvestris in Sweden. *Scandinavian Journal of Forest Research*, *14*, 376–412. doi:10.1080/02827589950152700.

Borisjuk, L., Rolletschek, H., & Neuberger, T. (2012). Surveying the plant's world by magnetic resonance imaging. *The Plant Journal*, *70*, 129–146. doi:10.1111/j.1365-313X.2012.04927.x PMID:22449048.

Brüchert, F., Baumgartnert, R., & Sauter, U. H. (2008). *Ring width detection for industrial purposes – Use of CT and discrete scanning technology on fresh round wood*. Paper presented at the Conference COST E53. Delft, The Netherlands.

Bucur, V. (2003). *Nondestructive characterization and imaging of wood*. Berlin: Springer-Verlag. doi:10.1007/978-3-662-08986-6.

Bucur, V. (2006). *Acoustics of wood* (2nd ed.). Berlin, Germany: Springer-Verlag.

Chang, S. J., Olson, J. R., & Wang, P. C. (1989). NMR imaging of internal features in wood. *Forest Prod J*, *39*(6), 43–49.

Coates, E. R., Chang, S. J., & Liao, W. (1998). A quick defect detection algorithm for magnetic resonance images of hadrwood logs. *Forest Products Journal*, *48*(10), 68–74.

Contreras, I., Guesalaga, A., Fernández, M. P., Guarini, M., & Irarrázaval, P. (2002). MRI fast tree log scanning with helical under sampled projection acquisitions. *Magnetic Resonance Imaging*, *20*, 781–787. doi:10.1016/S0730-725X(02)00602-1 PMID:12591574.

Cown, D. J., & Clement, B. C. (1983). A wood densitometer using direct scanning with X-rays. *Wood Science and Technology*, *17*(2), 91–93. doi:10.1007/BF00369126.

De Graaf, R. A. (2007). *In vivo NMR spectroscopy principles and techniques* (2nd ed.). West Sussex, UK: Wiley. doi:10.1002/9780470512968.

Dvinskikh, S. V., Henriksson, M., Berglund, L. A., & Furó, I. (2011). A multinuclear magnetic resonance imaging (MRI) study of wood with adsorbed water: Estimating bound water concentration and local wood density. *Holzforschung*, *65*, 103–107. doi:10.1515/hf.2010.121.

EARTO. (2012). *CT log scanner gives forestry industry the inside story on maximising value*. Retrieved January 10, 2013 from http://www.earto.eu/fileadmin/content/03_Publications/2012CS_SP.pdf

Eitelberger, J., Hofstetter, K., & Dvinskikh, S. V. (2011). A multi-scale approach for simulation of transient moisture transport processes in wood below the fiber saturation point. *Composites Science and Technology*, *71*, 1727–1738. doi:10.1016/j.compscitech.2011.08.004.

Ekstedt, J., Rosenkilde, A., Hameury, S., Sterley, M., & Berglind, H. (2007). *Measurement of moisture content profiles in coated and uncoated scots pine using magnetic resonance imaging*. Paper presented at COST E 53 Conference - Quality Control for Wood and Wood Products. Warsaw, Poland.

Flibotte, S., Menon, R. S., MacKay, A. L., & Hailey, J. R. T. (1990). Proton magnetic resonance of western red cedar. *Wood Fiber Sci*, *22*(4), 362–376.

Funt, B., & Bryant, E. C. (1987). Detection of internal log defects by automatic interpretation of computer tomography images. *Forest Product Journal*, *37*(1), 56–62.

Geya, Y., Kimura, T., Fujisaki, H., Terada, Y., Kose, K., & Haishi, T. et al. (2013). Longitudinal NMR parameter measurements of Japanese pear fruit during the growing process using a mobile magnetic resonance imaging system. *Journal of Magnetic Resonance*, *226*, 45–51. doi:10.1016/j.jmr.2012.10.012 PMID:23211549.

Gierlik, E., & Muchorowska, M. (2000). Some remarks on gamma-densitometry of wood. In F. Divos (Ed.), *12th International Symposium on Nondestructive Testing of Wood* (pp. 245-250). Sopron, Hungary: University of Western Hungary.

Grabianowski, M., Manley, B., & Walker, J. C. (2006). Acoustic measurements on standing trees, logs and green lumber. *Wood Science and Technology*, *40*, 205–216. doi:10.1007/s00226-005-0038-5.

Hall, L. D., Rajanayagam, V., Stewart, W. A., & Steiner, P. R. (1986). Magnetic resonance imaging of wood. *Canadian Journal of Research*, *2*, 423–426.

Harless, T. E. G., Wagner, F. G., Steele, P. H., Taylor, F. W., Yadama, V., & McMillin, C. (1991). Methodology for locating defects within hardwood and determining their impact on lumber value yield. *Forest Products Journal*, *41*(4), 25–30.

Hashemi, R. H., Bradley, W. G., & Lisanti, C. J. (2004). *MRI The basics* (2nd ed.). Philadelphia: Lippincott Williams & Wilkins.

Haygreen, J., & Bowyer, J. (1996). *Forest products and wood science: An introduction* (3rd ed.). Ames, IA: Iowa State University Press.

Homan, N. M., Windt, C. W., Vergeldt, C. W., Gerkema, E., & Van As, H. (2007). 0.7 and 3 T MRI and sap flow in intact trees: Xylem and phloem in action. *Applied Magnetic Resonance*, *32*, 157–170. doi:10.1007/s00723-007-0014-3.

Ilvonen, K., Palva, L., Perämäki, M., Joensuu, R., & Sepponen, R. (2001). MRI-based D2O/H2O-contrast method to study water flow and distribution in heterogeneous systems: Demonstration in wood xylem. *Journal of Magnetic Resonance*, *149*, 36–44. doi:10.1006/jmre.2001.2284.

IUFRO Division 5 – Forest Products. (2012). *5.02.01 – Non-destructive evaluation on wood and wood-based materials*. Retrieved November 15, 2012, from http://www.iufro.org/science/divisions/division-5/50000/50200/50201/

James, W. L., Yen, Y., & King, R. J. (1985). *A microwave method for measuring moisture content, density, and grain angle of wood*. Research Note FPL-0250. Washington, DC: United State Department of Agriculture, Forest Service, Forest Products Laboratory.

Johansson, J., Hagman, O., & Oja, J. (2003). Predicting moisture content and density of Scots pine by microwave scanning of sawn timber. *Methods*, *41*, 85–90.

Jones, M., Aptaker, P. S., Cox, J., Gardiner, B. A., & McDonald, P. J. (2012). A transportable magnetic resonance imaging system for in situ measurements of living trees: The tree hugger. *Journal of Magnetic Resonance*, *218*, 133–140. doi:10.1016/j.jmr.2012.02.019 PMID:22445351.

Kak, A. C., & Slaney, M. (1988). *Principles of computerized tomographic imaging*. IEEE Press.

Karsulovic, J. T., Dinator, M. I., Morales, P., Gaete, V., & Barrios, A. (2005). Determinación del diámetro del cilindro central defectuoso en trozas podadas de pino radiata (pinus radiata) mediante atenuación de radiación gamma. *Bosque*, *26*(1), 109–122.

Kimura, T., Geya, Y., Terada, Y., Kose, K., Haishi, T., Gemma, H., & Sekozawa, Y. (2011). Development of a mobile magnetic resonance imaging system for outdoor tree measurements. *The Review of Scientific Instruments*, *82*(5), 053704. doi:10.1063/1.3589854 PMID:21639504.

Kuroda, K., Kanbara, Y., Inoue, T., & Ogawa, A. (2006). Magnetic resonance micro-imaging of xylem sap distribution and necrotic lesions in tree stems. *Iowa J*, *27*(1), 3–17. doi:10.1163/22941932-90000133.

Leininger, T. D., Schmoldt, D. L., & Tainter, F. H. (2001). Using ultrasound to detect defects in trees: Current knowledge and future needs. In *Proceedings of the First International Precision Forestry Cooperative Symposium* (pp. 99-107). Seattle, WA: College of Forest Resources, University of Washington, USDA Forest Service.

Li, L., Wang, X., Wang, L., & Allison, R. B. (2012). Acoustic tomography in relation to 2D ultrasonic velocity and hardness mappings. *Wood Science and Technology*, *46*, 551–561. doi:10.1007/s00226-011-0426-y.

Llanos, C., Landau, D., Fernández, M. P., Guesalaga, A., Irarrázaval, P., & Tejos, C. (2010). Análisis de aspectos morfológicos y defectos de la madera de Pinus radiata D. Don por medio de resonancia nuclear magnética (MRI). In *Proceedings of the V Congreso Chileno de Ciencias Forestales*. Temuco, Universidad Católica de Temuco, Escuela de Ciencias Forestales.

Longuetaud, F., Mothe, F., Kerautret, B., Krähenbühl, A., Hory, L., Leban, J. M., & Debled–Rennesson, I. (2012). Automatic knot detection and measurement from X-ray CT images of wood: A review and validation of an improved algorithm on soft-wood samples. *Computers and Electronics in Agriculture*, *85*, 77–89. doi:10.1016/j.compag.2012.03.013.

MacMillan, M. B., Schneider, M. H., Sharp, A. R., & Balcom, B. J. (2001). Magnetic resocance imaging of water concentration in low moisture content wood. *Wood and Fiber Science*, *34*(2), 276–286.

Mahon, J. M. Jr, Jordan, L., Schimleck, L. R., Clarck, A. III, & Daniels, R. F. (2009). A comparison of sampling methods for a standing tree acoustic device. *South. J. Appl. For.*, *33*(2), 62–68.

Meder, R., Codd, S. L., Franich, R. A., Callaghan, P. T., & Pope, J. M. (2003). Observation of anisotropic water movement in Pinus radiata D. Don sapwood above fiber saturation using magnetic resonance micro-imaging. *Holz Roh Werkst*, *61*, 251–256. doi:10.1007/s00107-003-0400-y.

Menon, R. S., Mackay, A. L., Flibotte, S., & Hailey, J. R. T. (1989). Quantitative separation of NMR images of water in wood on the bases of T_2. *Journal of Magnetic Resonance*, *82*, 205–210.

Merela, M., Sepe, A., Oven, P., & Sersa, I. (2005). Three-dimensional in vivo magnetic resonance microscopy of beech (Fagus sylvatica L.) wood. *Magma*, *18*, 171–174. doi:10.1007/s10334-005-0109-5 PMID:16059737.

Moberg, L. (2000). Models of internal knot diameter for pinus sylvestris. *Scandinavian Journal of Forest Research*, *15*, 177–187. doi:10.1080/028275800750014984.

Morales, S., Guesalaga, A., Fernández, M. P., Guarini, M., & Irarrázaval, P. (2004). Computer reconstruction of pine tree rings using MRI. *Magnetic Resonance Imaging*, *22*, 403–412. doi:10.1016/j.mri.2004.01.015 PMID:15062936.

Müller, U., Bammer, R., Halmschlager, E., Stollberger, R., & Wimmer, R. (2001). Detection of fungal wood decay using magnetic resonance imaging. *Holz Roh Werkst*, *59*, 190–194. doi:10.1007/s001070100202.

Nishimura, D. G. (1996). *Principles of magnetic resonance imaging*. Palo Alto, CA: Stanford University Press.

Novelline, R., & Squire, L. (2004). *Squire's fundamentals of radiology* (6th ed.). Boston: Harvard University Press.

Oja, J. (2000). Evaluation of knot parameters measured automatically in CT-images of Norway spruce (picea abies (L.) karst.). *Holz als Roh-und Werkstoff*, *58*, 375–379. doi:10.1007/s001070050448.

Oja, J., & Temnerud, E. (1999). The appearance of resin pocket in CT images of Norway spruce (picea abies (L.) Karst). *Holz als Roh-und Werkstoff*, *57*, 400–406. doi:10.1007/s001070050368.

Okada, F., Handa, S., Tomiha, S., Kose, K., Haishi, T., Utsuzawa, S., & Togashi, K. (2006). *Development of a portable MRI for outdoor measurements of plants*. Paper presented at the 6th Colloquium on Mobile Magnetic Resonance. Aachen, Germany.

Olson, J. R., Chang, S. J., & Wang, P. C. (1990). Nuclear magnetic resonance imaging: A noninvasive analysis of moisture distributions in white oak lumber. *Canadian Journal of Research*, *20*(5), 586–591. doi:10.1139/x90-076.

Oven, P., Merela, M., Mikac, U., & Serša, I. (2011). Application of 3D magnetic resonance microscopy to the anatomy of woody tissues. *IAWA Journal*, *32*(4), 401–414.

Pearce, R. B. (2000). Decay development and its restriction in trees. *Journal of Arboriculture*, *26*(1), 1–11.

Pearce, R. B., Fisher, B. J., Carpenter, T. A., & Hall, L. D. (1997). Water distribution in fungal lesions in the wood of sycamore, acer pseudoplatanus, determined gravimetrically and using nuclear magnetic resonance imaging. *The New Phytologist*, *135*(4), 675–688. doi:10.1046/j.1469-8137.1997.00688.x.

Pearce, R. B., Sümer, S., Doran, S. J., Carpenter, T. A., & Hall, L. D. (1994). Non-invasive imaging of fungal colonization and host response in the living sapwood of sycamore (acer pseudoplatanus L.) using nuclear magnetic resonance. *Physiological and Molecular Plant Pathology*, *45*, 359–384. doi:10.1016/S0885-5765(05)80065-7.

Prince, J. L., & Links, J. M. (2006). *Medical imaging: signals and systems* (2nd ed.). Englewood Cliffs, NJ: Prentice Hall.

Quick, J. J., Hailey, J. R. T., & Mackay, A. L. (1990). Radial moisture profiles of cedar sapwood during drying – A proton magnetic-resonance study. *Wood Fiber Sci*, *22*, 404–412.

Raczkowski, J., Lutomoski, K., Molinski, W., & Wos, R. (1999). Detection of early stages of wood decay by acoustic emission technique. *Wood Science and Technology*, *33*, 353–358. doi:10.1007/s002260050121.

Rojas, E. G., Hernández, R. E., Condal, A., Verret, D., & Beauregard, R. (2005). Exploration of the physical properties of internal characteristics of sugar maple logs and relationships with CT images. *Wood and Fiber Science*, *37*(4), 591–604.

Rojas, G., & Ortiz, O. (2012). Identificación del cilindro nudoso en imágenes TC de trozas podadas de Pinus radiata: Estudio comparativo. *Maderas. Ciencia y Tecnología*, *13*(1), 65–77. doi:10.4067/S0718-221X2012000100006.

Rosenkilde, A., & Glover, P. (2002). High resolution measurements of the surface layer moisture content during drying of wood using a novel magnetic resonance imaging technique. *Holzforschung*, *56*, 312–317. doi:10.1515/HF.2002.050.

Ross, R. J., Brashaw, B. K., & Pellerin, R. F. (1998). Non destructive evaluation of wood. *Forest Products Journal*, *48*(1), 14–19.

Sarigul, E., Abbott, A. L., & Schmoldt, D. L. (2003). Rule-driven defects detection in CT images of hardwood logs. *Computers and Electronics in Agriculture*, *41*, 107–119. doi:10.1016/S0168-1699(03)00046-2.

Schajer, G. S., & Orhan, F. B. (2005). Microwave non-destructive testing of wood and similar orthotropic materials. *Subsurface Sensing Technologies and Applications*, *6*(4), 293–313. doi:10.1007/s11220-005-0014-z.

Steele, P. H., Harless, T. E. G., Wagner, F. G., Kumar, L., & Taylor, F. W. (1994). Increased lumber value from optimum orientation of internal defects with respect to sawing pattern in hardwood sawlogs. *Forest Products Journal*, *44*(3), 69–72.

Steele, P. H., Wades, M. V., Bullard, S. H., & Araman, P. A. (1992). Relative kerf and sawing variation values some hardwood sawing machines. *Forest Products Journal*, *42*(2), 33–39.

Taylor, F. W., Wagner, F. G. Jr, & McMillin, C. W. (1984). Locating knots by industrial tomography- A feasibility study. *Forest Products Journal*, *34*(5), 42–46.

Terskikh, V. V., Feurtado, J. A., Ren, C., Abrams, S. R., & Kermode, A. R. (2005). Water uptake and oil distribution during imbibition of seeds of western white pine (pinus monticola dougl. ex D. don) monitored in vivo using magnetic resonance imaging. *Planta*, *221*, 17–27. doi:10.1007/s00425-004-1426-z PMID:15605241.

Tiitta, M., Olkkonen, H., Lappalainen, T., & Kanko, T. (1996). Density measurement of particleboard, veneer and wood specimens by narrow beam gamma absorption technique. In J. L. Sandoz (Ed.), *10th International Symposium on Nondestructive Testing of Wood* (pp. 187-200). Lausanne, France: Presses Polytechniques et Universitaires Romandes.

Umebayashi, T., Fukuda, K., Haishi, T., Sotooka, R., Zuhair, S., & Otsuki, K. (2011). The developmental process of xylem embolisms in pine wilt disease monitored by multipoint imaging using compact magnetic resonance imaging. *Plant Physiology*, *156*, 943–951. doi:10.1104/pp.110.170282 PMID:21505099.

Utsuzawa, S., Fukuda, K., & Sakaue, D. (2005). Use of magnetic resonance microscopy for the nondestructive observation of xylem cavitation caused by pine wilt disease. *Phytopathology*, *95*(7), 737–743. doi:10.1094/PHYTO-95-0737 PMID:18943004.

Van Has, H., & van Duynhoven, J. (2013). MRI of plants and foods. *Journal of Magnetic Resonance*. DOI:http://dx.doi.org/10.1016/j.jmr.2012.12.019

Van Houts, J. H., Wang, S., Shi, H., Pan, H., & Kabalka, G. W. (2004). Moisture movement and thickness swelling in oriented strandboard, part 1: Analysis using nuclear magnetic resonance micro imaging. *Wood Science and Technology*, *38*, 617–628. doi:10.1007/s00226-004-0258-0.

Veres, J. S., Cofer, G. P., & Johnson, G. A. (1991). Distinguishing plant tissues with magnetic resonance microscopy. *American Journal of Botany*, *78*, 1704–1711. doi:10.2307/2444849.

Wagner, F. G., Taylor, F. W., Ladd, D. S., McMillin, C. W., & Roder, F. L. (1989). Ultrafast CT scanning of an oak for internal defects. *Forest Products Journal*, *39*(11/12), 62–64.

Wang, P. C., & Chang, S. J. (1986). Nuclear magnetic resonance imaging of wood. *Wood Fiber Sci*, *18*, 308–314.

Wang, X., Verrill, S., Lowell, E., Ross, R., & Herian, V. (2009). Acoustic sorting models for log segregation. In H. Zhang & X. Wang (Eds.), *Proceedings of the 16th International Symposium on Nondestructive Testing And Evaluation of Wood* (pp. 45-51). Beijing, China: Beijing Forestry University.

Wei, Q., Zhang, S. Y., Chui, Y. H., & Leblon, B. (2009). Reconstruction of 3D images of internal log characteristics by means of successive 2D log computed tomography images. *Holzforschung*, *63*, 575–580. doi:10.1515/HF.2009.089.

Zhu, D., Conners, R. W., Schmoldt, D. L., & Araman, P. A. (1996). A prototype vision system for analyzing CT imagery of hardwood logs. *IEEE Transactions on Systems, Man, and Cybernetics. Part B, Cybernetics*, *26*(4), 522–532. doi:10.1109/3477.517028 PMID:18263051.

ADDITIONAL READING

Bucur, V. (2003). *Nondestructive characterization and imaging of wood*. Berlin: Springer-Verlag. doi:10.1007/978-3-662-08986-6.

Funt, B. V., & Bryant, E. C. (1987). Detection of internal logs defects by automatic interpretation of computer tomography images. *Forest Products Journal*, *37*(1), 56–62.

Hashemi, R. H., Bradley, W. G. Jr, & Lisanti, C. J. (2010). *MRI: The basics*. Philadelphia: Walters Kluwer-Lippincott Williams & Wilkins.

Liang, Z.-P., & Lauterbur, P. C. (1999). *Principles of magnetic resonance imaging: A signal processing perspective*. IEEE Press. doi:10.1109/9780470545652.

Oja, J. (2000). Evaluation of knot parameters measured automatically in CT-images of Norway spruce (picea abies (L.) karst.). *Holz als Roh un Werkstoff, 58*, 375-379.

Schmoldt, D., Scheinman, E., Rinnhofer, A., & Occeña, L. (2000). Internal log scanning: research to reality. In D.A. Meyer (Ed.), *Proceedings of the Twenty-Eighth Annual Hardwood Symposium: West Virginia Now-The Future for the Hardwood Industry?* (pp. 103-114). Memphis, TN: National Hardwood Lumber Association.

Schmoldt, D. L., He, J., & Abbot, A. L. (2000). Automated labelling of log feature in CT imagery of multiple hardwood species. *Wood and Fiber Science*, *32*(3), 287–300.

Seeram, E. (2001). *Computed tomography: Physical principles, clinical applications, and quality control*. Philadelphia: W.B. Saunders Company.

KEY TERMS AND DEFINITIONS

Attenuation: Attenuation is a general term that refers to any reduction in the strength of a signal. Sometimes called loss, attenuation is a natural consequence of signal transmission over long distances. In the case of CT scan, the attenuation is defined as the reduction of the flow intensity of radiation, for which at the moment that the flow naughty the object, some photons are absorbed and others get lost. The attenuation depends on the coefficient of attenuation of the material that forms the object.

CT Image: An image CT is formed for rectangular or square adjustment of the elements of the image (pixel), where every pixel represents the coefficient of attenuation equivalent to the volume of the pixel.

CT Scan (X-Rays Computed Tomography): CT scan is a medical imaging procedure that utilizes computer-processed X-rays to produce tomographic images or 'slices' of specific areas of the body. These cross-sectional images are used for diagnostic and therapeutic purposes in various medical disciplines. This technique non-destructive also has been used for evaluation on wood and wood-based materials.

Excitation: Delivering (inducing, transferring) energy into the "spinning" nuclei via radio-frequency pulse(s), which puts the nuclei into a higher energy state. Several excited nuclei can produce a net transverse magnetization, which can be then measured by a MRI scanner.

Knots: A knot is a particular type of imperfection in a piece of wood; it will affect the technical properties of the wood, usually for the worse, but may be exploited for visual effect. In a longitudinally sawn plank, a knot will appear as a roughly circular "solid" piece of wood around which the grain of the rest of the wood "flows" Within a knot, the direction of the wood (grain direction) is up to 90 degrees different from the grain direction of the regular wood. In the tree a knot is either the base of a side branch or a dormant bud. A knot, when the base of a side branch is conical in shape.

Magnetic Resonance: The absorption or emission of energy by atomic nuclei in an external magnetic field after the application of Radio Frequency (RF) excitation pulses using frequencies which satisfy the conditions of the Larmor equation.

Magnetic Resonance Imaging: (**MRI**) or **Nuclear Magnetic Resonance Imaging** (**NMRI**): Is a scanning devise originally designed for medical application

that is used to visualize internal structures of the body or other samples in a non-destructive way. It is based on the presence of hydrogen protons in the body or the sample, and the alignment and precession of those protons using constant, linearly varying and rotating magnetic fields.

Nuclear Spin: Also known as inherent spin, this defines the intrinsic property of certain nuclei (those with odd numbers of protons and/or neutrons in their nucleus) to exhibit angular momentum and a magnetic moment.

Proton Density: The concentration of mobile Hydrogen atoms within a sampled region.